Atmospheric Environment 320 (2024) 120315

Contents lists available at ScienceDirect

Atmospheric Environment

journal homepage: www.elsevier.com/locate/atmosenv

Reducing southern California ozone concentrations in the year 2050 under a low carbon energy scenario

Yusheng Zhao [a], Yin Li [b,c], Yiting Li [a], Anikender Kumar [b,d], Qi Ying [e], Michael J. Kleeman [b,*]

[a] Department of Land, Air And Water Resource, University of California, Davis, CA, 95616, USA
[b] Department of Civil and Environmental Engineering, University of California, Davis, CA, 95616, USA
[c] Department of Earth System Science, Tsinghua University, Beijing, China
[d] India Meteorological Department, New Delhi, India
[e] Zachry Department of Civil Engineering, Texas A&M University, College Station, TX, 77843, USA

HIGHLIGHTS

- O_3 violations will continue in Los Angeles even after adoption of low carbon fuels.
- VOC sources that contribute to future O_3 formation are not practical to control.
- Additional NOx reductions of 80% may be needed to reduce O_3 to safe levels.
- Public health benefits from aggressive NOx control are $30B/yr.

ARTICLE INFO

Keywords:
Ozone apportionment
CTM
NOx control
Ozone chemical regime
BenMap

ABSTRACT

Recent studies predict that ozone (O_3) concentrations within major California cities in the year 2050 will continue to violate the 8-h O_3 standard despite the adoption of low-carbon energy. This O_3 penalty largely stems from persistent NOx-rich chemistry within urban cores that causes O_3 concentrations to increase when traditional combustion sources are replaced by renewable energy sources. Here we employ a Chemical Transport Model (CTM) equipped with a novel O_3 source apportionment technique to better understand O_3 formation and to design supplemental control measures to complement Greenhouse Gases (GHG) reduction strategies in California. Two base scenarios were analyzed: (i) a 2050 "business-as-usual" (BAU) scenario with O_3 violations on 43% of simulated days, and (ii) a 2050 Greenhouse Gases reduction (GHGAi) scenario with O_3 violations on 32% of simulated days. The source apportionment results of the GHGAi scenario identified offroad equipment & rail, marine vessels & aircraft, and industrial & agricultural emissions as the major NOx sources that contributed to the O_3 violations, while boundary conditions & initial conditions (BCIC) and biogenic emissions were identified as the major volatile organic compounds (VOCs) sources. Despite a HCHO/NO2 ratio (FNR) suggesting that the SoCAB is in a VOC-limited chemical regime, the major VOC sources that contribute to O_3 formation are not controllable. Therefore, complementary O_3 control strategies are proposed that focus on NOx emissions within the GHGAi scenario. Three cumulative Supplemental Control Steps were evaluated. Control Step I reduced emissions from off-road equipment & rail, and marine vessels & aircraft (65% NOx emissions reduction relative to GHGAi). Control Step II expanded the measures in Control Step I by reducing emissions from industrial and agricultural sources (cumulative 73.6% NOx emissions reduction relative to GHGAi), while Control Step III extended the amount of control applied to all sources covered in Control Steps I and II (cumulative 85.4% NOx emissions reduction relative to GHGAi). All three Control Steps lowered O_3 concentrations significantly in the SoCAB, with residual O_3 violations mainly predicted in non-populated wilderness areas. The significant reductions in O_3 produced by the Supplemental Control Steps decreased the predicted incidence of hay fever/rhinitis, asthma, and all-cause mortality by an order of magnitude compared to the transformation from the BAU to GHGAi scenario. The predicted public health savings associated with the Supplemental Control Steps are valued at $19.70–30.36B/yr.

* Corresponding author.
E-mail address: mjkleeman@ucdavis.edu (M.J. Kleeman).

https://doi.org/10.1016/j.atmosenv.2023.120315
Received 8 September 2023; Received in revised form 14 December 2023; Accepted 18 December 2023
Available online 23 December 2023

1. Introduction

Global efforts to mitigate the most harmful effects of climate change have gradually strengthened, with 196 parties of the United Nations Framework Convention on Climate Change (UNFCCC) agreeing to cut GHG emissions by 43% by 2030 (UNFCCC, 2015). Progressive cities and states with sufficient economic resources have also developed their own climate action plans. California has a long-standing commitment to a clean environment and a top 10 world economy, California therefore has both the motivation and the resources to take a leadership role on climate change. Assembly Bill 32 (passed in 2006) commits California to reducing GHG emissions by 80% of 1990 levels by the year 2050 (California Air Resources Board, 2006). Much of this reduction will be achieved through a transformation of the energy system towards renewable sources that emit little or no GHGs.

Transforming energy infrastructure is expensive, and many of the climate benefits will not be realized for decades. Immediate air quality co-benefits may make this transformation more attractive in the near term. Zapata et al. (2018b) and Li et al. (2022b) analyzed the air quality benefits associated with curbing GHG emissions in California and concluded that the immediate public health savings from reduced air pollution exceeded $20B/yr, significantly offsetting the economic costs. Internal analysis conducted by staff at the California Air Resources Board confirms these findings (California Air Resources Board, 2022). Much of this public health saving is associated with reduced concentrations of airborne particulate matter ($PM_{2.5}$). The other major component of photochemical smog, ozone (O_3), does not respond as beneficially to programs that reduced GHG emissions due to the predicted increases of O_3 concentrations in urban areas. The South Coast Air Basin (SoCAB) in California is the only designated area in the United States where O_3 design values have exceeded 100 ppb for the past ten years (USEPA, 2023). Anthropogenic emissions in the SoCAB have been significantly reduced over the past four decades (Wu et al., 2023) leading to a long-term trend of declining O_3 concentrations, but recent progress has been more limited and O_3 design values started increasing again after 2016. Numerous measurement studies and model studies have analyzed the present-day trends (Perdigones et al., 2022; Wu et al., 2021, 2023; Zhu et al., 2019) to support the creation of near-term control programs based on a weight of evidence approach. Similar efforts are needed for future scenarios that adopt low-carbon fuels.

Simulations of future conditions in the year 2050 with reduced GHG emissions predict that O_3 concentrations would continue to violate the National Ambient Air Quality Standards (NAAQS) in major California cities (Zapata et al., 2018a). Additional controls are therefore needed to address this future residual air quality problem. Here we conducted air quality simulations in California for the year 2050 using a chemical transport model (CTM) configured with a new O_3 source apportionment technique to assist in the development of future O_3 mitigation plans that are compatible with GHG emissions reduction goals. NOx and volatile organic compound (VOC) source contributions to O_3 concentrations are quantified in the basecase scenario that focuses exclusively on GHG emissions reductions. Supplemental control programs are then designed that focus on the sources of NOx and VOC that make the largest contributions to O_3 concentrations. Multiple control scenarios are analyzed with increasingly stringent controls to achieve compliance with the O_3 NAAQS. The public health benefits associated with each supplemental control program are estimated using established epidemiological relationships. The results of this study proactively develop solutions to anticipated air quality problems as California undertakes an energy transformation to address climate change.

2. Methods

2.1. Model description

Air quality in the year 2050 was simulated using the University of California Davis/California Institute of Technology (UCD/CIT) air quality model configured with a new O_3 source apportionment technique. The UCD/CIT model is a 3-D source-oriented regional chemical transport model optimized for source tagging of primary and secondary air pollution (Kleeman and Cass, 2001; Yu et al., 2019). Performance statistics for O_3 and PM concentrations predicted by the UCD/CIT model meet the generally accepted criteria (Emery et al., 2017) for chemical transport models (Hu et al., 2015; Venecek et al., 2018, 2019; Ying et al., 2008; Yu et al., 2019; Zhao et al., 2022). Most recently, Zhao et al. (2022) found that the O_3 performance of the UCD/CIT model is comparable to the performance of the CMAQ model developed by the US EPA. The UCD/CIT model has flexible solution algorithms that allow new chemical mechanisms to be tested with minimal effort. Two versions of the SAPRC11 chemical mechanism (Carter and Heo, 2013) were used to describe the gas-phase chemical reactions in the current study. The first version of the mechanism was configured to track NOx source-contributions to O_3 while the second version was configured to track VOC source-contributions (Zhao et al., 2022).

UCD/CIT calculations were carried out over two domains in the current study (Fig. S1). The outer domain covered the entire state of California with a resolution of 24 km, and the inner domain covered Southern California with a resolution of 4 km. The area with the bold outline in Fig. S1 marks the boundary of the SoCAB, which is the primary focus area in the current study where O_3 concentrations exceed the standards designed to protect public health. The vertical domain extended 5 km above the earth's surface using 16 telescoping layers with a height of 30 m in the first layer. Multiple studies have demonstrated that this configuration is suitable for air quality predictions in California (Hu et al., 2014a, 2014b, 2015; Venecek et al., 2019; Yu et al., 2019).

Air quality simulations were conducted for 32 weeks randomly selected from 2046 to 2055 to properly represent inter-annual variability associated with the El Nino Southern Oscillation (ENSO) cycle. Eight (8) weeks were designated in each of the four seasons to ensure representative coverage throughout the year. This unbiased randomized sampling approach characterizes both the long-term average and the variability in pollutant concentrations without the computational expense of simulating every day in the 10-year window. Future meteorological fields were generated using the Weather Research and Forecasting model (WRFv3.4). Initial and boundary conditions for WRF simulations were generated using results from the Community Climate System Model (CCSM) under the representative concentration pathways (RCP) 8.5, which is a high GHG-emission (worst-case) scenario.

Future emissions for criteria air pollutants were generated by the CA-REMARQUE_v1.0 model, which will be discussed in detail in Section 2.2. Initial and boundary conditions for air quality simulations were based on predictions from the Model for Ozone and Related chemical Tracers (MOZART) for historical years, assuming that the initial and boundary conditions in 2050 will be fixed and similar to current conditions.

2.2. Future emissions

Future emission scenarios have been described in detail by Zapata et al. (2018a) and Li et al. (2022a) and so only a brief summary is provided here. Two economically optimized energy scenarios were constructed for California in the year 2050 using the energy-economic optimization model, CA-TIMES. One scenario was a "business-as-usual" case (BAU) that incorporated current policy regulations to achieve the goals outlined in California Assembly Bill 32 (AB32). This scenario defines conditions when 2020 GHG emissions are limited to 1990 levels, but no extra efforts are taken to move toward a low-carbon society beyond 2020. The second scenario explored aggressive greenhouse gas mitigation strategies (GHGAi) that achieved an 80% reduction of GHG emissions relative to year 1990 by the year 2050 using deep penetration of advanced technologies and renewable energies. NOx emissions in the GHGAi scenario are ~25% lower than the BAU scenario. The NOx reductions are mainly from "off-road equipment and railway", and

"residential and commercial buildings". VOC emissions do not change significantly, with only 2.8% reduction from BAU to GHGAi.

Both energy scenarios were used as inputs to the CA-REMARQUE_v1.0 model to generate corresponding emissions for criteria air pollutants. Emissions were grouped into nine source sectors: tire and break wear, on road vehicles, off-road equipment and rail, marine vessels and aircraft, residential and commercial buildings, electricity generation, fuel supply, industrial and agricultural, and biogenic emissions (Li et al., 2022a, 2022b).

2.3. O_3 source apportionment technique

The O_3 source apportionment technique applied in the UCD/CIT model has been fully described by Zhao et al. (2022). The SAPRC11 chemical mechanism was expanded into two versions that tag O_3 precursors, intermediate products, and final O_3 concentrations. The first tagged version of the UCD/CIT model is a NOx source apportionment (NOx SA) method. This version tags the nitrogen atoms contained in NOy species NO, NO_2, NO_3, N_2O_5, HNO_3, HNO_4, PAN, etc., and tracks NOx source contributions to O_3 formation. In addition to the nitrogen atoms, O^3P, O^1D, and O_3 are also tagged to pass the source apportionment information from NOy species to O_3.

The second tagged version of the UCD/CIT model is a VOC source apportionment (VOC SA) method. This version tags odd-oxygen and tracks VOC source contributions to O_3 formation from different groups. Each VOC tag is then passed to the peroxy radicals and other compounds containing odd oxygen produced in the chemical reactions, which will finally go to O_3 and other sink species. It should be noted that tagging methods are purely an accounting exercise to track O_3 source contributions. The total concentrations (summed across all sources) of the species predicted by the NOx SA and VOC SA variants of the UCD/CIT model are equivalent.

2.4. Emission reductions

Several emission reduction strategies are proposed based on the O_3 source apportionment results. Source sectors that contribute strongly to O_3 formation are prioritized for reductions. A formal cost analysis was not undertaken, but the cumulative emissions controls were generally configured in order of increasing reductions. We used the 3rd highest MD8H O_3 across the simulated 32 weeks (rank 3 out of 224 days) as criterion to assess O_3 violations. This percentile is approximately equivalent to the annual 4th highest MD8H O_3 in a year (rank 4 out of 365 days), known as the design value classified by the US EPA. The ambient O_3 concentrations predicted under each emissions control were evaluated before the next control stage was implemented.

2.5. Health benefits

The health benefits associated with O_3 reductions were calculated using the Environmental Benefits Mapping and Analysis Program – Community Edition (BenMAP-CE) v1.5.8.22 developed by the US EPA. The health functions used in the analysis are listed in Table S1, including Incidence of Asthma (Garcia et al., 2019), Incidence of Hay Fever/-Rhinitis (Parker et al., 2009), and All-Cause Mortality (Turner et al., 2016). Average MD8H O_3 concentrations under the BAU scenario, the GHGAi scenario, and the Control Steps of the GHGAi scenario were used to calculate the health impacts associated with different scenarios and control strategies. This calculation uses the default BenMAP population data that is projected to 2050 by Woods & Poole (Woods & Poole Economics Inc, 2015).

3. Results and discussion

3.1. O_3 violation in future scenarios

Among the 32 simulated weeks (224 days), MD8H O_3 concentrations exceeded 70 ppb on 101 days under the BAU scenario and 71 days under the GHGAi scenario (see Table 1). The 3rd highest MD8H O_3 plots for the BAU and the GHGAi scenarios are shown in Fig. 1. The 70 ppb O_3 standard is significantly exceeded in the SoCAB under both emissions scenarios, which is consistent with the findings in Zapata et al. (2018a). The maximum O_3 exceedance across all grid cells is 22.5 ppb in the BAU scenario, placing the SoCAB in the Moderate nonattainment category for the 2015 8-h O_3 standard. The O_3 exceedance in the GHGAi scenario is 16.1 ppb, placing the SoCAB in the Moderate nonattainment category as well. O_3 violations occur in these future scenarios because reductions in NOx emissions are insufficient to fully shift the atmosphere into the NOx-limited chemical regime in the year 2050. More aggressive and targeted NOx emissions controls are described in the following sections.

3.2. O_3 source contributions under the GHGAi scenario

Source contributions to the 3rd highest MD8H O_3 concentrations under the GHGAi scenario are shown in Figs. 2 and 3. "Offroad equipment & rail", and "marine vessels & aircraft" are the two major NOx emission groups that contribute to O_3 violations (Fig. 2). Emissions from "off-road equipment & rail" form 16–26.3 ppb of O_3. NOx emissions from "marine vessels & aircraft" form 20–35 ppb of O_3. "Industrial & agricultural emissions" are the third largest O_3 contributor among the NOx emission groups, forming 8–14 ppb of O_3 in the region. NOx emissions from "residential & commercial buildings" and "electricity generation" each contribute to smaller amounts of O_3 formation (<7 ppb each). NOx emissions from on road vehicles and fuel supply make very small contributions to O_3 concentrations (<2.4 ppb each). It should be noted that "boundary & initial conditions (BCICs)" are a major source of O_3 in the NOx source apportionment simulation in the San Diego region, but not in the SoCAB. This reflects the proximity of San Diego to the computational boundary.

VOC SA results (Fig. 3) predict that BCICs play an important role in the central portion of the SoCAB with the 3rd highest O_3 concentration. Background O_3 and VOC concentrations contribute approximately 50 ppb of O_3 in the SoCAB, making BCICs the single largest O_3 "source" in the VOC SA calculations. BCIC contributions are even higher in the northeastern portion of the model domain, although this region has slightly lower total O_3 concentrations. Biogenic VOC emissions are the next most significant O_3 source, forming 10–21 ppb of O_3 in the central portion of the SoCAB. VOC emissions from "industrial & agricultural sources" contribute to approximately 10 ppb of O_3 formation. VOC emissions from "off-road equipment & rail", and "marine vessels & aircraft" contribute to 2.49–6.16 ppb and 1.4–4.63 ppb of O_3 formation, respectively. Contributions from the other VOC sources are very small and negligible.

The formaldehyde to NO_2 ratio (FNR) is often used as an indicator of the chemical regime for O_3 formation (NOx-limited vs. VOC-limited). Fig. 4 illustrates the FNR plots under the BAU and the GHGAi scenarios. A threshold of FNR = 4.6 is used as the transition between the

Table 1
Number of days with O3 exceeding 70 ppb.

	BAU	GHGAi	GHGAi with Control Step I	GHGAi with Control Step II	GHGAi with Control Step III
Total days of simulation	224	224	140	56	35
Days of exceedance	101	71	26	21	13

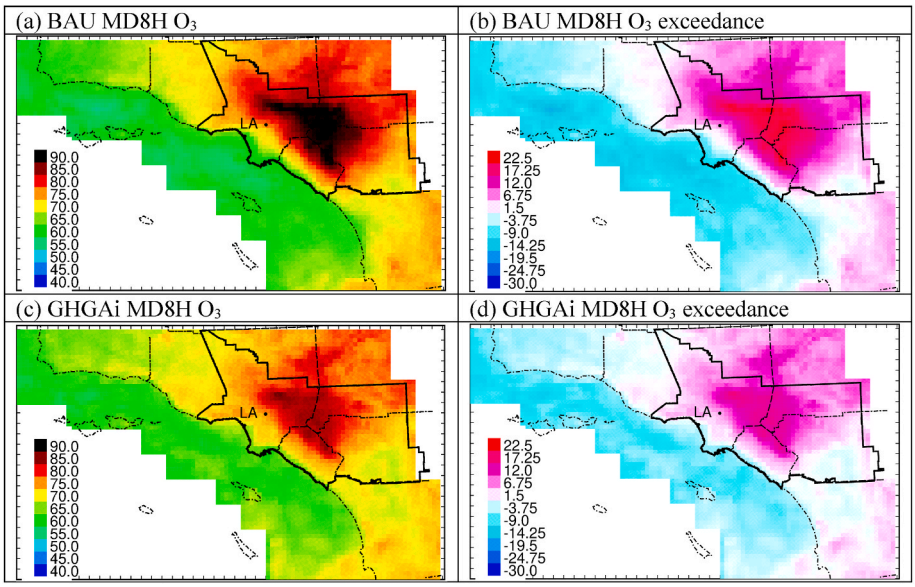

Fig. 1. 3rd highest MD8H O_3 and exceedance (vs. 70 ppb), unit: ppb.

NOx-limited and VOC-limited chemical regimes (Wu et al., 2021). Grid cells with positive values (red) are NOx-limited, and grid cells with negative values (blue) are VOC-limited. In both scenarios, regions that violate the 70-ppb standard are mostly VOC-limited. O_3 chemistry in the SoCAB has historically been in the VOC-limited regime (Jin et al., 2020). Recent studies have stated that the basin is transitioning to NOx-limited conditions, and may have been NOx-limited on average during spring and summer of 2020 (Perdigones et al., 2022; Schroeder et al., 2022). Direct chamber measurements of ambient O_3 sensitivity present a more complex picture, with significant days still VOC-limited (Wu et al., under review). However, considering that the major VOC sources that contribute to O_3 formation in the SoCAB are BCICs and biogenic emissions, it is more practical to reduce the anthropogenic emissions of the major NOx sources.

3.3. Emissions reduction

Several emissions reduction strategies were investigated to reduce O_3 concentrations in future years. Results from three cumulative levels of emissions controls are described in the following sections.

3.3.1. Emissions Control Step I

NOx emissions controls were first applied to the two largest O_3 contributors: "off-road equipment & rail", and "marine vessels & aircrafts". In the "off-road equipment and railroad" emission sector, we assume adoption of electricity or some other power source that does not emit NOx in future years. Emissions in this sector are therefore reduced to zero.

Future emissions of NOx from marine vessels were reduced by 80% based on future compliance with the International Convention for the Prevention of Pollution from Ships (MARPOL) Annex VI Tier III standard. The original marine vessel emissions in the GHGAi scenario were based on 2010 levels (Zapata et al., 2018b) placing them in Annex VI Tier I. We assume an average lifespan for an ocean vessel is $\leq$ 30 years. Therefore, by the year of 2050, all in-use ocean vessels should comply with the Annex VI Tier III standard, with emissions reduced by 80% compared to Tier I. Total NOx and None-Methane VOC (NMVOC) emissions in the SoCAB decrease by 65% and 15.5% relative to the GHGAi scenario, respectively.

Fig. 5(a) and (b) show the 3rd highest MD8H O_3 concentrations and O_3 exceedance under Emissions Control Step I. O_3 concentrations are significantly reduced across the SoCAB, and a large portion of the O_3 violation disappears under the enhanced emissions controls. O_3 concentrations are reduced by a maximum of 18.9 ppb in Control Step I (Fig. S5(a)). The reductions in the 3rd highest O_3 concentrations under Control Step I are sufficient to move the SoCAB from Moderate to Marginal non-attainment status.

Fig. S2 shows the NOx SA results for the Control Step I. Emissions from "offroad equipment & rail" are reduced to zero in this scenario and so these sources no longer contribute to O_3 formation. NOx emissions from marine vessels are reduced by 80%, greatly reducing their contribution to O_3 formation in coastal areas. Residual NOx emissions from "marine vessels and aircraft" still contribute up to 30.2 ppb of O_3 formation in the inland regions of the SoCAB.

3.3.2. Emissions Control Step II

The remaining O_3 violations under Emissions Control Step I have significant source contributions from industrial and agricultural sources. Additional cumulative measures in Control Step II reduce emissions from industrial and agricultural sources by 50% through the adoption of low-NOx engines similar to those used in the on-road fleet. Total NOx and NMVOC emissions in the SoCAB decrease by 73.6% and 15.5% relative to the GHGAi scenario, respectively.

Fig. 5(c) and (d) show the 3rd highest MD8H O_3 plots and O_3 exceedance under Emissions Control Step II. The region that experiences O_3 violations inside the SoCAB shrinks under Control Step II, with one grid cell near Redlands and several grid cells at the northeastern boundary continuing to exceed 70 ppb. However, the region outside the SoCAB that experiences O_3 violations is relatively unchanged by these control measures. Fig. S5(b) shows that the basin-wide O_3 reduction from Control Step I to Step II is less than 5 ppb. Some areas show very small O_3 increases (<0.2 ppb) due to decreased NOx emissions in the NOx-rich chemical regime that exists at those locations (Fig. 6(b)).

3.3.3. Emissions Control Step III

Emissions Control Step III applies more aggressive controls in an attempt to further reduce ambient O_3 concentrations. NOx emissions from marine vessels are reduced by 90% instead of 80%, and NOx emissions from the industrial and agricultural sectors are completely removed with the assumption that these sources will be electrified. Off-road equipment and rail remain at zero emissions. Total NOx and NMVOC emissions in the SoCAB decrease by 85.4% and 15.5% relative to the GHGAi scenario, respectively. The cost and feasibility of these emissions controls are not evaluated in the current study, but this case

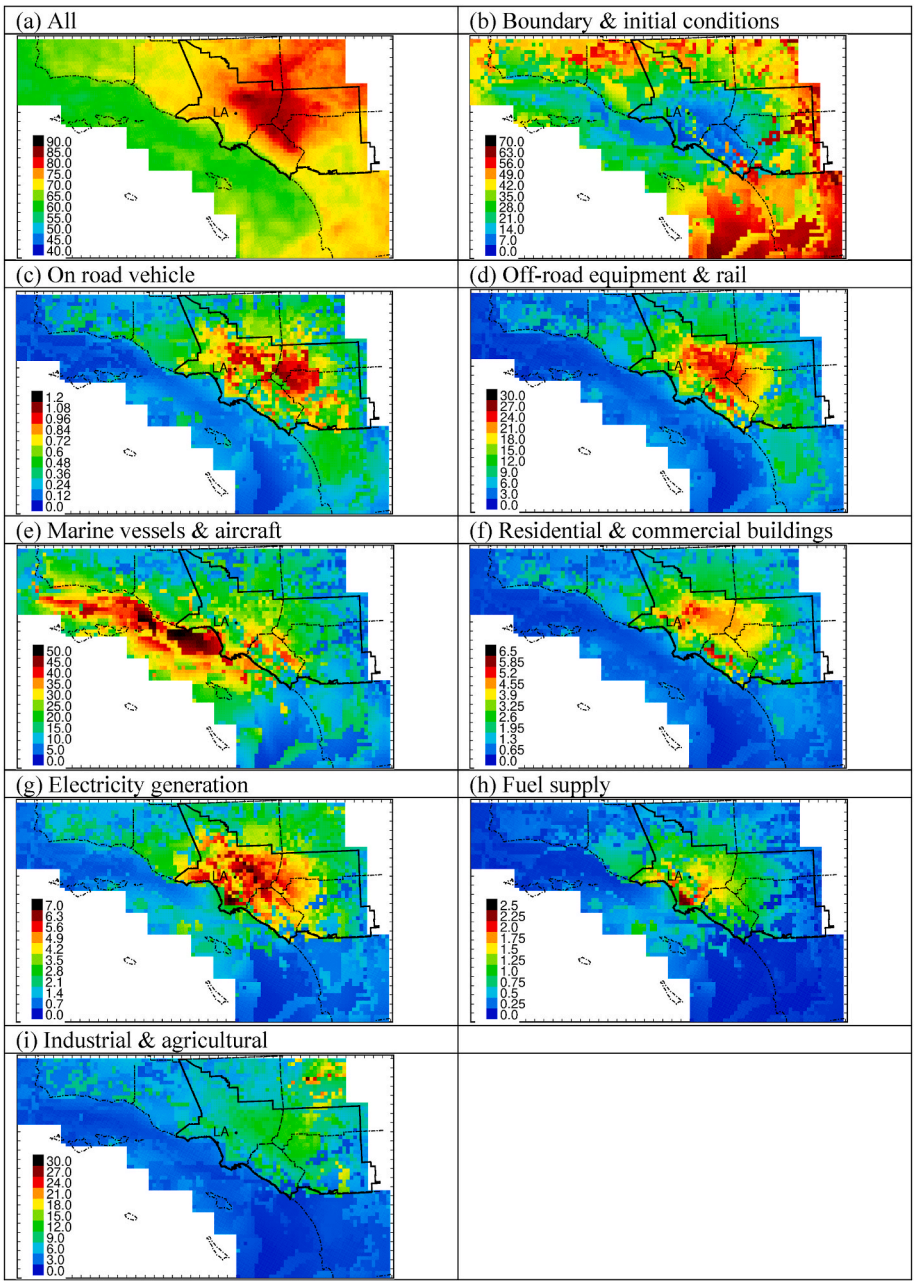

Fig. 2. NOx Source Contributions to 3rd highest MD8H O_3 in GHGAi, unit: ppb.

illustrates the limiting behavior of the system.

Fig. 5(e) and (f) show the 3rd highest MD8H O_3 and O_3 exceedance under Emissions Control Step III. With the more stringent control measures in the Control Step III, O_3 concentrations are basically below 70 ppb across the SoCAB. The remaining few grid cells with minor exceedance are located at non-populated wilderness areas, which should not represent a widespread public health risk. Similarly, the region with O_3 violations outside the SoCAB also shrinks under Emissions Control Step III.

3.4. Health benefits

Fig. 7 shows the 32-week average MD8H O_3 concentration predicted under the BAU, GHGAi, and the three GHGAi control step scenarios used in the BenMAP calculations. Domain-wide calculations of the health benefits based on the averaged MD8H O_3 in Southern California are shown in Fig. 8 and Table S2. Each health benefit is expressed relative to a reference case. GHGAi-BAU uses the BAU scenario as the reference case. StepI-GHGAi, StepII-GHGAi, and StepIII-GHGAi each use the GHGAi scenario as the reference case. In Fig. 8, the health benefits were shown as the percentage of the highest health benefits of the three controls. Each health benefit is proportional to the changes in O_3 concentrations, and so the distribution of benefits across scenarios looks similar. The baseline supplemental controls in Step I reduced incidence of hay fever/rhinitis and asthma by a factor of 8.2 and reduced total mortality by a factor of 11.4 relative to the GHGAi-BAU health benefits. The most stringent controls in Step III reduced the incidence of hay fever/rhinitis and asthma being a factor of 12.3 and the reduced total mortality being a factor of 17.5 relative to the GHGAi-BAU health benefits. The public-health present-day value of these controls are estimated at $19.70–30.36B/yr using a value of a statistical life equal to $7.6 M. These public health savings should be considered when weighing the costs of each control measure.

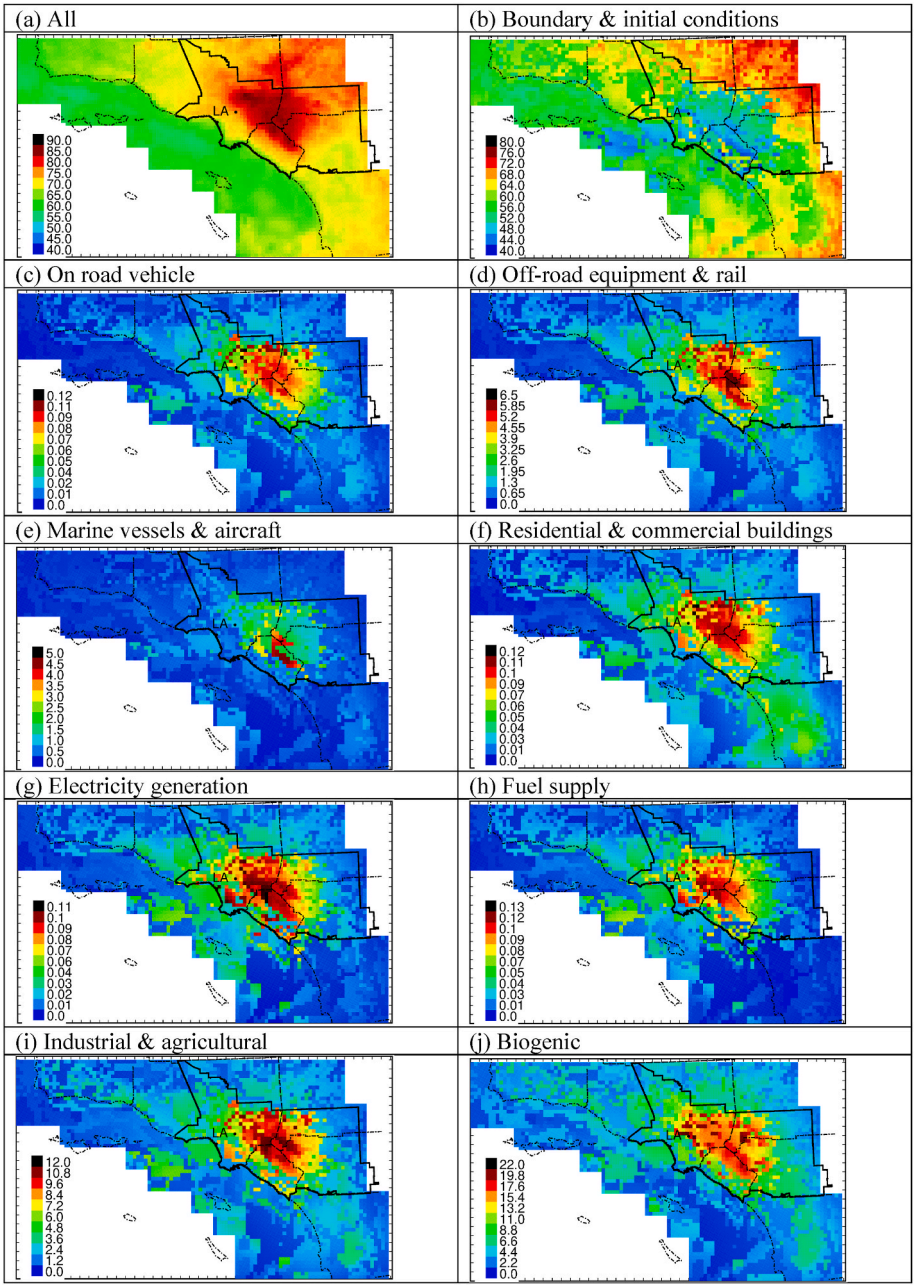

Fig. 3. VOC Source Contributions to 3rd highest MD8H O_3 in GHGAi, unit: ppb.

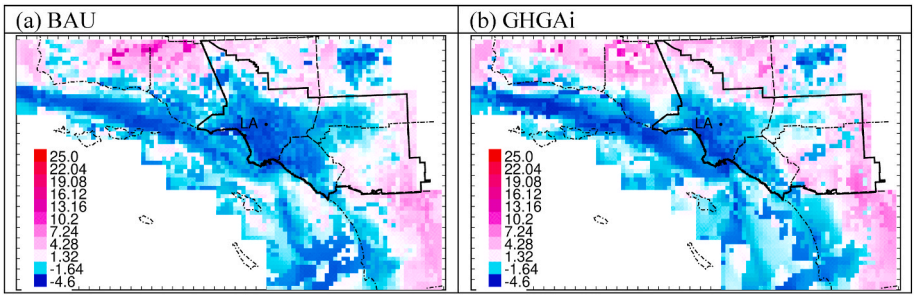

Fig. 4. HCHO/NO_2 (FNR) for the corresponding 3rd highest MD8H O_3 days.

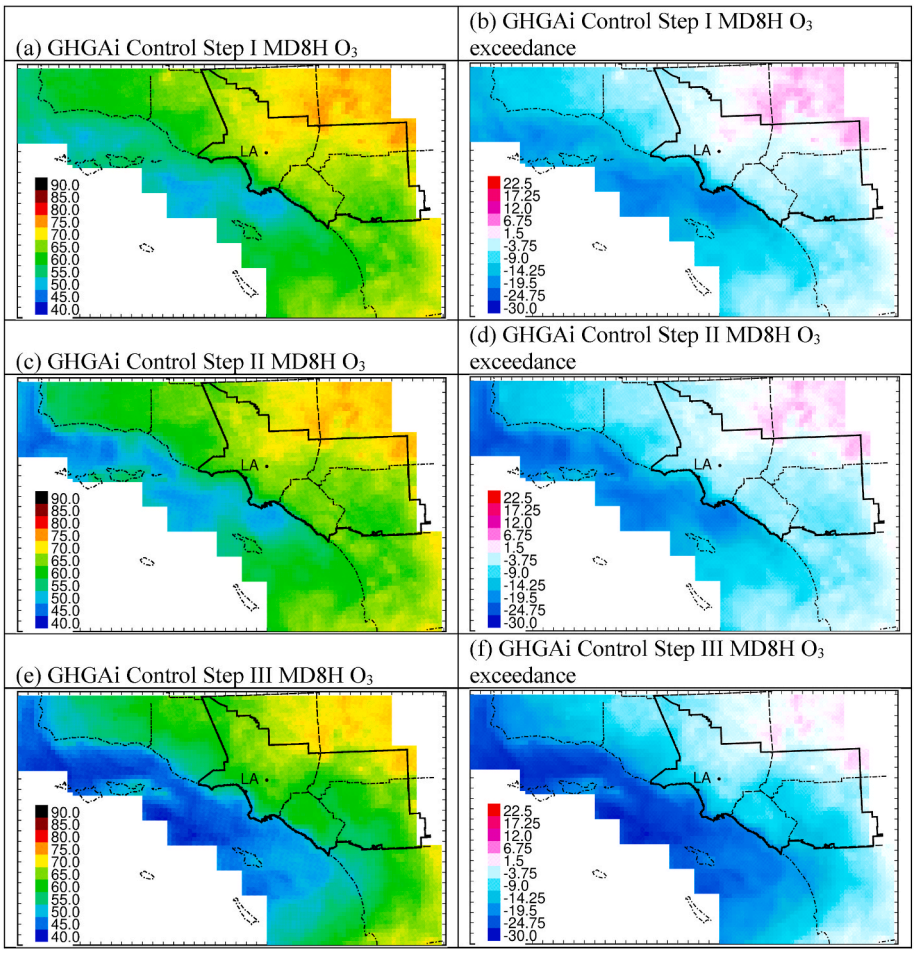

Fig. 5. 3rd highest MD8H O_3 and exceedance (vs. 70 ppb) in different emission control steps, unit: ppb.

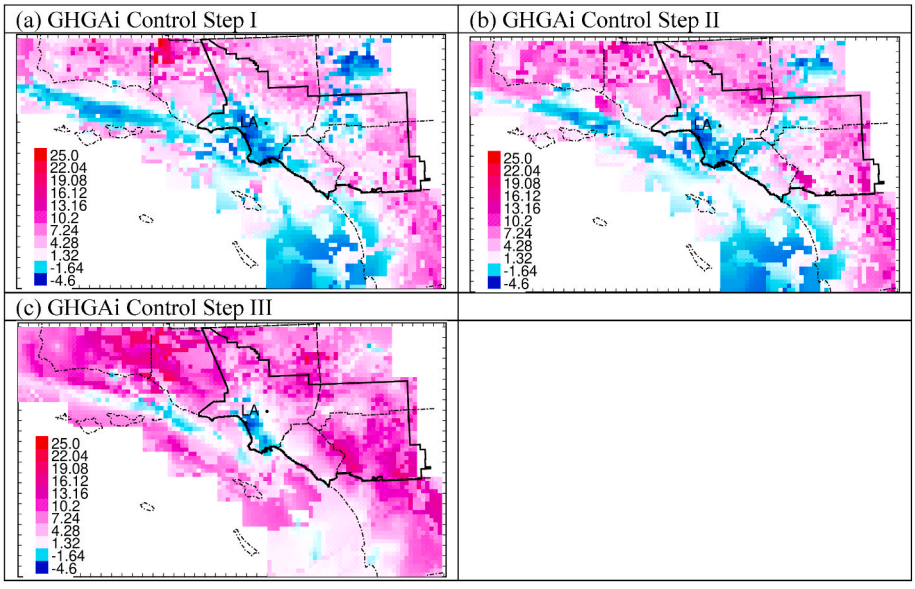

Fig. 6. HCHO/NO_2 (FNR) for the corresponding 3rd highest MD8H O_3 days in different control steps.

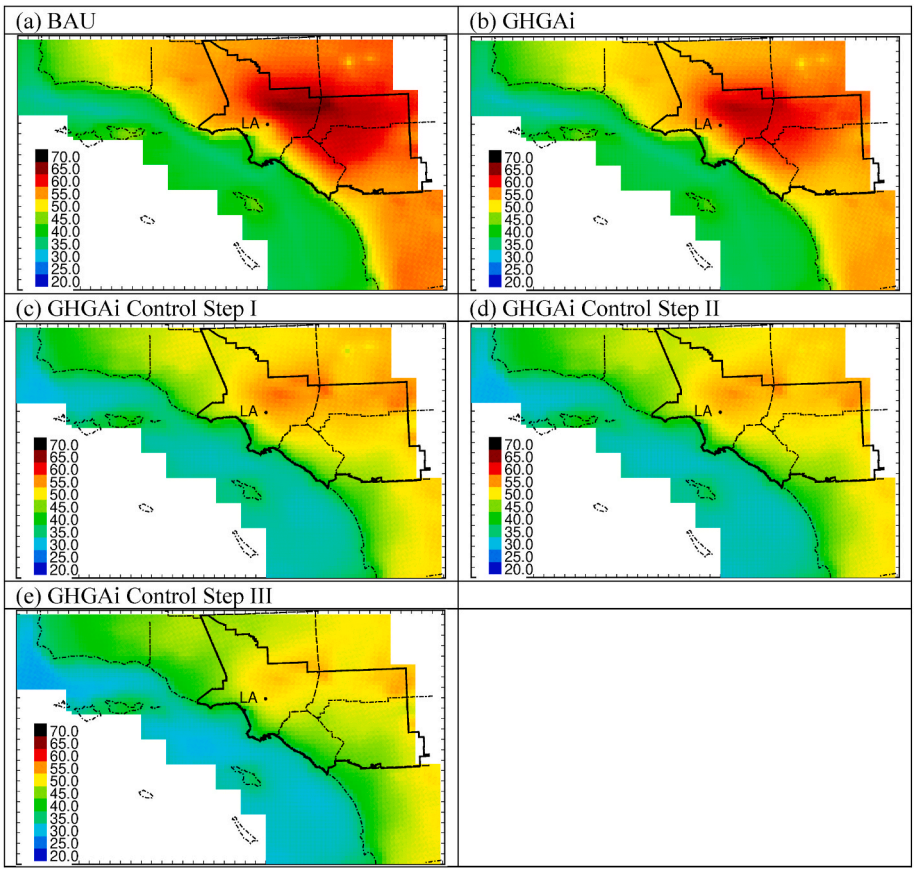

Fig. 7. 32-week average MD8H O_3 plots in all scenarios, unit: ppb.

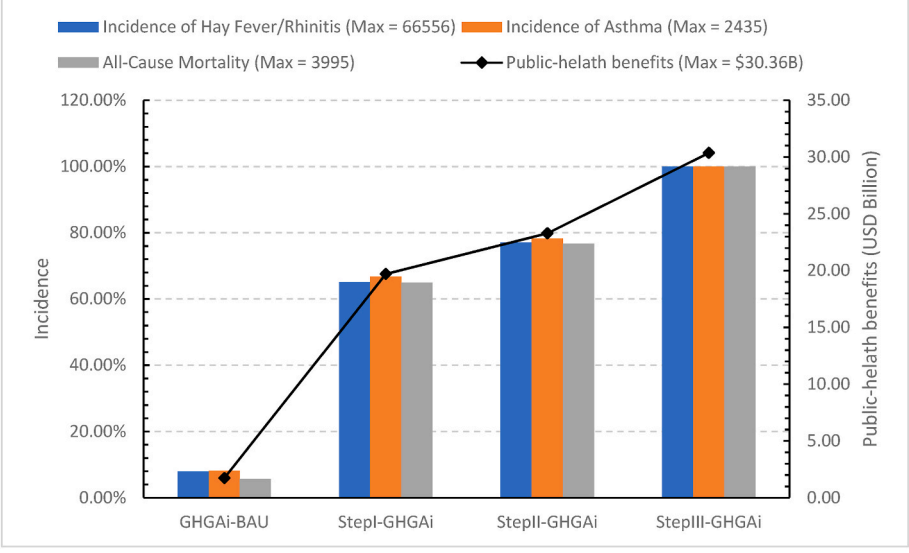

Fig. 8. Health benefits in different scenarios.

4. Conclusion

Air quality simulations for Southern California in the year 2050 under a Business as Usual (BAU) and GHG reduction (GHGAi) scenario predict continued violations of the current 8-h O_3 standard despite significant reductions in $PM_{2.5}$ mass concentrations. These O_3 violations largely stem from persistent NOx-rich chemistry in urban cores that produces higher O_3 concentrations as combustion sources are replaced by renewable energy sources. A new O_3 apportionment technique was used to identify emission sources that contribute to the high O_3 concentrations in the SoCAB in the year 2050. Major VOC sources that contribute to O_3 formation include biogenic emissions within the study area and upwind sources outside the study area, meaning that local VOC controls will not be effective at reducing high O_3 concentrations in the year 2050. Major NOx sources that contribute to O_3 formation include "off-road equipment & rail", "marine vessels & aircraft", and "industrial

& agricultural emissions". Each of these sources could be controlled to reduce O_3 concentrations.

Three cumulative emission control strategies were designed to reduce NOx emissions that contribute to O_3 formation in the SoCAB in the year 2050 under a reduced GHG emissions case. Control Step I reduced emissions from "offroad equipment and rail" to zero and reduced emissions from marine vessels by 80% leading to a 53% reduction in regional NOx emissions. The maximum O_3 exceedance for the 3rd highest MD8H O_3 decreased from 16.1 ppb to 5.1 ppb, shifting the non-attainment status of the basin from Moderate to Marginal. Control Step II reduced emissions from "industrial and agricultural sources" by 50% leading to a 64% reduction in regional NOx emissions. O_3 violations near the city of Los Angeles disappeared under Control Step II, but exceedances still occurred near Redlands and at other locations to the northeast of Los Angeles. A more aggressive Control Step III was tested that reduced the NOx emissions from marine vessels by 90% and eliminated the NOx emissions from the industrial and agricultural sources (offroad equipment and rail emissions remain at zero) produced an 80% reduction in regional NOx emissions. Control Step III reduced O_3 concentrations below 70 ppb throughout the SoCAB except for a few unpopulated mountainous locations.

The three control steps reduced hay fever/rhinitis, asthma, and all-cause mortality in the SoCAB. Control Step 1 improved health benefits by a factor of 9.3 relative to the reduced GHG emissions scenario, while Control Step III improved health benefits by a factor of 14.1 relative to the reduced GHG emissions scenario. The public health savings associated with these control measures are estimated to be $19.70–30.36B/yr.

The sources identified for emissions reduction in Control Steps I, II, and II release emissions in California but they are not necessarily subject to current California regulations. Controls on international and interstate goods movement and agricultural engines will require planning and coordination with other governing agencies. Some of these emissions controls may also require the development or deployment of new power sources to replace traditional combustion system. Each of these efforts will take decades to implement. Identifying sources of O_3 formation now provides the necessary planning timeline to address this key element of photochemical smog formation in California.

CRediT authorship contribution statement

Yusheng Zhao: Writing – original draft. **Yin Li:** Formal analysis. **Yiting Li:** Formal analysis. **Anikender Kumar:** Formal analysis. **Qi Ying:** Writing – review & editing. **Michael J. Kleeman:** Conceptualization, Formal analysis, Methodology, Project administration, Supervision, Validation, Writing – original draft.

Declaration of competing interest

The authors declare that they have no known competing financial interests or personal relationships that could have appeared to influence the work reported in this paper.

Data availability

Data will be made available on request.

Acknowledgements

This study was partially funded by the California Air Resources Board under Contract No. 15AQP010 and the United States Environmental Protection Agency under Grant No. R83587901. The statements and conclusions in this report are those of the contractor and not necessarily those of the California Air Resources Board. The mention of commercial products, their source, or their use in connection with material reported herein is not to be construed as actual or implied endorsement of such products. Although the research described in the article has been funded by the United States Environmental Protection Agency it has not been subject to the Agency's required peer and policy review and therefore does not necessarily reflect the reviews of the Agency and no official endorsement should be inferred.

Appendix A. Supplementary data

Supplementary data to this article can be found online at https://doi.org/10.1016/j.atmosenv.2023.120315.

References

California Air Resources Board, 2022. 2022 Scoping Plan for Achieving Carbon Neutrality.

California Air Resources Board, 2006. AB-32 Air Pollution: Greenhouse Gases: California Global Warming Solutions Act of 2006 [WWW Document]. URL. https://leginfo.legislature.ca.gov/faces/billNavClient.xhtml?bill_id=200520060AB32. (Accessed 28 June 2023).

Carter, W.P.L., Heo, G., 2013. Development of revised SAPRC aromatics mechanisms. Atmos. Environ. 77, 404–414. https://doi.org/10.1016/j.atmosenv.2013.05.021.

Emery, C., Liu, Z., Russell, A.G., Odman, M.T., Yarwood, G., Kumar, N., 2017. Recommendations on statistics and benchmarks to assess photochemical model performance. J. Air Waste Manag. Assoc. 67, 582–598. https://doi.org/10.1080/10962247.2016.1265027.

Garcia, E., Berhane, K.T., Islam, T., McConnell, R., Urman, R., Chen, Z., Gilliland, F.D., 2019. Association of changes in air quality with incident asthma in children in California, 1993-2014. JAMA, J. Am. Med. Assoc. 321, 1906–1915. https://doi.org/10.1001/jama.2019.5357.

Hu, J., Zhang, H., Chen, S., Ying, Q., Wiedinmyer, C., Vandenberghe, F., Kleeman, M.J., 2014a. Identifying PM 2.5 and PM 0.1 sources for epidemiological studies in California. Environ. Sci. Technol. 48, 4980–4990. https://doi.org/10.1021/es404810z.

Hu, J., Zhang, H., Chen, S.H., Wiedinmyer, C., Vandenberghe, F., Ying, Q., Kleeman, M. J., 2014b. Predicting primary PM 2.5 and PM 0.1 trace composition for epidemiological studies in California. Environ. Sci. Technol. 48, 4971–4979. https://doi.org/10.1021/es404809j.

Hu, J., Zhang, H., Ying, Q., Chen, S.H., Vandenberghe, F., Kleeman, M.J., 2015. Long-term particulate matter modeling for health effect studies in California - Part 1: model performance on temporal and spatial variations. Atmos. Chem. Phys. 15, 3445–3461. https://doi.org/10.5194/acp-15-3445-2015.

Jin, X., Jin, X., Fiore, A., Fiore, A., Boersma, K.F., Boersma, K.F., Smedt, I. De, Valin, L., 2020. Inferring changes in summertime surface ozone-NOx-VOC chemistry over U.S. Urban areas from two decades of satellite and ground-based observations. Environ. Sci. Technol. 54, 6518–6529. https://doi.org/10.1021/acs.est.9b07785.

Kleeman, M.J., Cass, G.R., 2001. A 3D Eulerian source-oriented model for an externally mixed aerosol. Environ. Sci. Technol. 35, 4834–4848. https://doi.org/10.1021/es010886m.

Li, Yin, Yang, C., Li, Yiting, Kumar, A., Kleeman, M.J., 2022a. Future emissions of particles and gases that cause regional air pollution in California under different greenhouse gas mitigation strategies. Atmos. Environ. 273, 118960 https://doi.org/10.1016/j.atmosenv.2022.118960.

Li, Yiting, Kumar, A., Li, Yin, Kleeman, M.J., 2022b. Adoption of low-carbon fuels reduces race/ethnicity disparities in air pollution exposure in California. Sci. Total Environ. 834, 155230 https://doi.org/10.1016/j.scitotenv.2022.155230.

Parker, J.D., Akinbami, L.J., Woodruff, T.J., 2009. Air pollution and childhood respiratory allergies in the United States. Environ. Health Perspect. 117, 140–147. https://doi.org/10.1289/ehp.11497.

Perdigones, B.C., Lee, S., Cohen, R.C., Park, J.H., Min, K.E., 2022. Two decades of changes in summertime ozone production in California's South Coast Air Basin. Environ. Sci. Technol. 56, 10586–10595. https://doi.org/10.1021/acs.est.2c01026.

Schroeder, J.R., Cai, C., Xu, J., Ridley, D., Lu, J., Bui, N., Yan, F., Avise, J., 2022. Changing ozone sensitivity in the South Coast Air Basin during the COVID-19 period. Atmos. Chem. Phys. 22, 12985–13000. https://doi.org/10.5194/acp-22-12985-2022.

Turner, M.C., Jerrett, M., Pope, C.A., Krewski, D., Gapstur, S.M., Diver, W.R., Beckerman, B.S., Marshall, J.D., Su, J., Crouse, D.L., Burnett, R.T., 2016. Long-term ozone exposure and mortality in a large prospective study. Am. J. Respir. Crit. Care Med. 193, 1134–1142. https://doi.org/10.1164/rccm.201508-1633OC.

UNFCCC, 2015. Paris Agreement [WWW Document]. URL. https://treaties.un.org/Pages/ViewDetails.aspx?src=TREATY&mtdsg_no=XXVII-7-d&chapter=27&clang=_en. (Accessed 24 July 2023).

USEPA, 2023. 2022 Design Value Reports [WWW Document]. URL. https://www.epa.gov/air-trends/air-quality-design-values. (Accessed 13 December 2023).

Venecek, M.A., Yu, X., Kleeman, M.J., 2019. Predicted ultrafine particulate matter source contribution across the continental United States during summertime air pollution events. Atmos. Chem. Phys. 19, 9399–9412. https://doi.org/10.5194/acp-19-9399-2019.

Venecek, M.A., Yu, X., Kleeman, M.J., 2018. Ultrafine particulate matter source contributions across the continental United States. Atmos. Chem. Phys. Discuss. 1–26. https://doi.org/10.5194/acp-2018-833.

Woods & Poole Economics Inc, 2015. Complete Demographic Database. Washington, DC [WWW Document]. URL. http://www.woodsandpoole.com/index.php.

Wu, K., Zhu, S., Mac Kinnon, M., Samuelsen, S., 2023. Unexpected deterioration of O3 pollution in the South Coast Air Basin of California: the role of meteorology and emissions. Environ. Pollut. 330, 121728 https://doi.org/10.1016/j.envpol.2023.121728.

Wu, S., Alaimo, C.P., Zhao, Y., Green, P.G., Young, T.M., Liu, S., Kuwayama, T., Coggon, M.M., Gilman, J.B., Robinson, A.M., Veres, P.R., Neuman, A., Kleeman, M.J., Under review. O3 sensitivity to NOx and VOC during RECAP-CA and its implication in the emission control strategy. Environ. Sci. Technol..

Wu, S., Lee, H.J., Rohrbacher, A., Liu, S., Kuwayama, T., Seinfeld, H., Kleeman, M.J., 2021. Direct measurements of ozone response to emissions perturbations in California. Atmos. Chem. Phys. Discuss. https://doi.org/10.5194/acp-2021-708.

Ying, Q., Lu, J., Allen, P., Livingstone, P., Kaduwela, A., Kleeman, M., 2008. Modeling air quality during the California Regional PM10/PM2.5 Air Quality Study (CRPAQS) using the UCD/CIT source-oriented air quality model - Part I. Base case model results. Atmos. Environ. 42, 8954–8966. https://doi.org/10.1016/j.atmosenv.2008.05.064.

Yu, X., Venecek, M., Kumar, A., Hu, J., Tanrikulu, S., Soon, S.T., Tran, C., Fairley, D., Kleeman, M.J., 2019. Regional sources of airborne ultrafine particle number and mass concentrations in California. Atmos. Chem. Phys. 19, 14677–14702. https://doi.org/10.5194/acp-19-14677-2019.

Zapata, C.B., Yang, C., Yeh, S., Ogden, J., Kleeman, M.J., 2018a. Low-carbon energy generates public health savings in California. Atmos. Chem. Phys. 18, 4817–4830. https://doi.org/10.5194/acp-18-4817-2018.

Zapata, C.B., Yang, C., Yeh, S., Ogden, J., Kleeman, M.J., 2018b. Estimating criteria pollutant emissions using the California Regional Multisector Air Quality Emissions (CA-REMARQUE) model v1 . 0. Geosci. Model Dev 11, 1293–1320. https://doi.org/10.5194/gmd-11-1293-2018.

Zhao, Y., Li, Y., Kumar, A., Ying, Q., Vandenberghe, F., Kleeman, M.J., 2022. Separately resolving NOx and VOC contributions to ozone formation. Atmos. Environ. 285, 119224 https://doi.org/10.1016/j.atmosenv.2022.119224.

Zhu, S., Horne, J.R., Mac Kinnon, M., Samuelsen, G.S., Dabdub, D., 2019. Comprehensively assessing the drivers of future air quality in California. Environ. Int. 125, 386–398. https://doi.org/10.1016/j.envint.2019.02.007.